ELSEVIER

PII: S0032-3861(96)01026-9

*Polymer* Vol. 38 No. 17, pp. 4311–4318, 1997

0032-3861/97/$17.00+0.00

# Deformation mechanism of polyethylene spherulites estimated by crystal orientation distribution function and small angle light scattering under Hv polarization condition

**Masaru Matsuo* and Chunye Xu**

*Department of Textile and Apparel Science, Faculty of Human Life and Environment, Nara Women's University, Nara 630, Japan*

*(Received 26 June 1996; revised 13 September 1996)*

The deformation mechanism of polyethylene spherulites was studied by using melt films of high density polyethylene with a 78% crystallinity in terms of crystallite orientation distribution estimated by X-ray diffraction technique and small angle light scattering under Hv polarization condition. In doing so, a model relating crystal orientation to the deformation of polyethylene spherulite was proposed. The distribution function of crystallites within a spherulite was assumed to be a function of crystal lamella. The distribution functions of reciprocal lattice vectors of given crystal planes were derived from two functions of the crystallites and lamellae with several parameters. The best values of each parameter were determined by the simplex method associated with direct research method to obtain the object function on the basis of trial and error. As a result, it was found that at an initial elongation ratio of 1.5, the most important factor in fitting the model to experimental results, was the preferred orientation of lamellar axis but most of the crystallites within the lamella were maintained without taking characteristic orientation. The Hv scattering from a deformed three-dimensional spherulite was formulated on the basis of the proposed model. The scattered intensity distribution in an undeformed state showed the typical four-leaf clover pattern and the lobes extending in the horizontal direction indicated the deformation of spherical to ellipsoid structure with a draw ratio of 1.5. The calculated patterns were in good agreement with those observed. © 1997 Elsevier Science Ltd.

**(Keywords: polyethylene spherulite; crystallite orientation distribution; small angle light scattering; reciprocal lattice vector; object function)**

## INTRODUCTION

The orientation mechanism of crystallites has been studied mainly for polyethylene. A number of quantitative investigations have been reported for a spherulitic structure by using essentially very similar models. Following the initial studies[1,2], the deformation of the spherulite was compared with that of the models in terms of the second order orientation factors of the orientation distribution functions of the principal crystallographic axes of the crystallites; $F_{20}^{j}$ ($j$ denoting $a$, $b$, and $c$ axes). The second order orientation factors provide, however, only limited knowledge of the orientation distribution and one cannot discuss the crystalline orientation in detail on this basis. Further studies were discussed by comparing the dependence of orientation distribution function of crystallites upon the extension ratio with that calculated from a spherulite deformation model which combines the crystal lamellar orientation in affine fashion with the reorientation of the crystal grains within the orienting lamellae[3–6]. The crystal reorientation mechanism was represented by two preferential fashions which involve rotations of the crystal grains about their own $a$ and $b$ axes so as to orient their $c$ axes toward the stretching direction[4–6]. These models have been proposed on the basis of morphological studies, for example, by Hay and Keller[7] using optical microscopy (polarized), electron microscopy, macro and micro X-rays, by Kobayashi and Nagasawa[8] using optical microscopy (polarized) and electron microscopy, and by Samuels[9] using small angle light scattering. In the proposed model systems, the distribution function of the orientation of crystallites within the lamellae was given as a function of lamellar orientation. The calculated functions of the reciprocal lattice vectors of the crystal planes took negative values at some regions of polar angle. This is probably due to the introduction of the term to cancel out the variation of a normalization constant of orientation function of crystallites within the lamella[4–6]. Without introducing this term, it was impossible to pursue theoretical calculations by using the simplex method which is a direct search method to obtain the object function on the basis of trial and error[10]. Recent development of computer can pursue the theoretical calculations without introducing the term. This paper is concerned with the analysis of crystal orientation within a spherulite by using the realistic model and analysis of small angle light scattering pattern under Hv polarization condition calculated on the basis of the model. Of course, a similar treatment

* To whom correspondence should be addressed

can be applied to the orientation of crystallites within a rod[11].

Apart from these geometrical treatments[3–6], a statistical treatment concerning oriented crystallization was proposed by Matsuo *et al.*[12] on the basis of the estimation of segmental orientation in deformed polymer networks using a lattice model similar to that by Erman *et al.*[13,14]. This treatment is basically related to the concept of Flory[15,16] associated with the preferred axis of a given domain along one of the principle axes of the lattice for a liquid crystal system and of hard rods dispersed in a dilute solution. This treatment, however, cannot explain the relationship between crystal and lamellar orientations. Accordingly, a model similar to the previous models[5,6] is again proposed to explain the deformation mechanism of a polyethylene spherulite clearly in terms of the relationship between crystallite and lamellar orientations.

## EXPERIMENTAL

A high density polyethylene, Sholex 5009, having a viscosity-average molecular weight, $M_v$, of $6.7 \times 10^4$ was used as a test specimen. The pellets of Sholex 5055 were melted at 180°C for 10 min in a laboratory press under a pressure of 0.2 GPa, slowly cooled to 80°C and annealed for 1 h. The film obtained was slowly cooled down to room temperature.

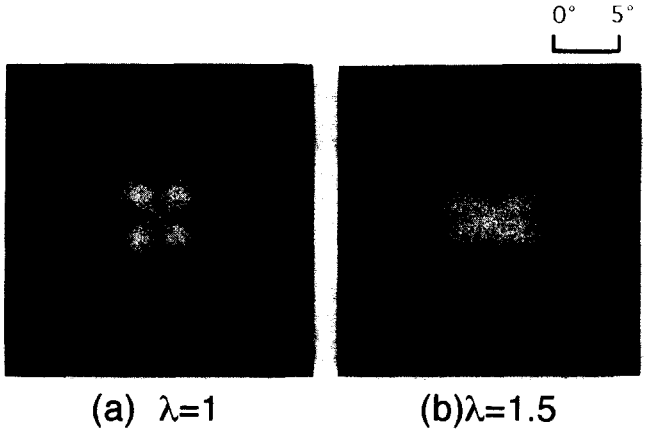


**Figure 1** Small angle light scattering patterns under Hv polarization condition (a) undeformed state, (b) deformed state ($\lambda = 1.5$)

Densities of the films were measured by a pycnometer using a mixture of chlorobenzene and toluene. The specimens were immersed in ethanol prior to measurements. The crystallinity was calculated by using 1.000 and 0.852 g cm$^{-3}$ as densities of the crystal and amorphous phases, respectively. The crystallinity of high density polyethylene was 78%.

Light scattering patterns were obtained with a 3 mW He–Ne gas laser as a light source. Diffuse surface were avoided by sandwiching the specimens between microcover glasses with a silicon immersion oil having a similar index.

The X-ray measurements were carried out with a 12 kW rotating-anode X-ray generator (Rigaku RDA-rA) operated at 200 mA and 40 kV.

The orientation distribution function of crystallites can be calculated on the basis of the orientation functions of the reciprocal lattice vectors measured by X-ray diffraction, according to the method proposed by Roe and Krigbaum[17–19]. Measurements of the X-ray diffraction intensity distribution were performed using a horizontal scanning type goniometer, operating at a fixed time-step scan of 0.1°/40 s over a range of twice the Bragg angle $2\theta_B$ from 15° to 60° and from 70° to 79°by rotating about the film normal direction at 2–5° intervals from 0° to 90°. The intensity distribution was measured as a function of a given rotational angle $\theta_j$, and the corrections of X-ray diffraction intensity were made for air scattering, background noise, polarization, absorption, incoherent scattering and amorphous contribution. The intensity curve thus obtained was assumed to be due to the contribution of the intensity from the crystalline phase. The intensity curve $I_{cry}(2\theta_B)$ was separated into the contribution from the individual crystal planes, assuming that each peak had a symmetric form given by a Lorenzian function in equation (1), where $I_j^0$ is the maximum intensity of the $j$th peak.

$$I_{cry}(2\theta_B) = \sum_j \frac{I_j^0}{1 + (2\theta_0^j - 2\theta_B)^2/\beta_j^2} \qquad (1)$$

Here $\beta_j$ is the half-width of the $j$th peak at half the peak intensity and $\theta_0^j$ is the Bragg angle at which the maximum intensity of the $j$th peak appears. Using the same process at a given $\theta_j$ in the range from 0° to 90°, the intensity distribution $I_j(\theta_j)$ can be determined

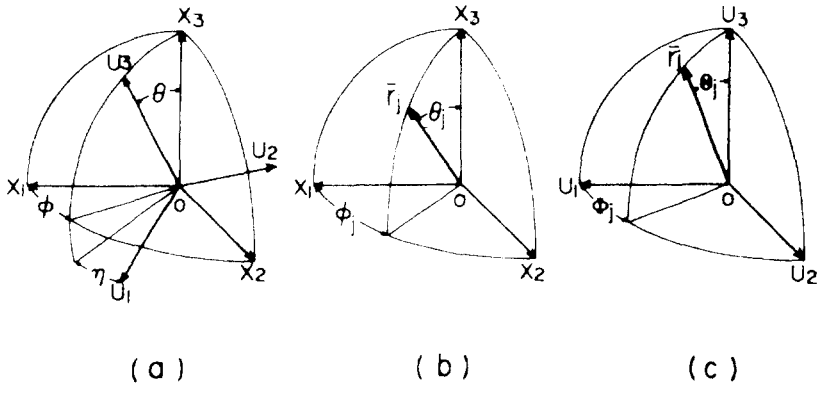


**Figure 2** Cartesian coordinate illustrating the geometrical relation. (a) Euler angles $\theta$ and $\eta$ which specify the orientation of coordinate $0-U_1U_2U_3$ of the structural unit with respect to coordinate $0-X_1X_2X_3$ of specimen. (b) Angles $\theta_j$ and $\phi_j$ which specify the orientation of the given $j$th axis of the structural unit with respect to the coordinate $0-X_1X_2X_3$. (c) Angles $\Theta_j$ and $\Phi_j$ which specify the orientation of the $j$th axis of the structural unit with respect to the coordinate $0-U_1U_2U_3$

for the respective $j$th plane, and the orientation distribution function of the $j$th reciprocal lattice vector may be given by

$$2\pi q_j(\cos\theta_j) = \frac{I(\theta_j)}{\int_0^{\pi/2} I(\theta_j)\sin\theta_j \,\mathrm{d}\theta_j} \tag{2}$$

## RESULTS AND DISCUSSION

*Figure 1* shows Hv light scattering patterns from the Sholex melt films. The pattern from the undrawn film is the so-called 'four leaf clover pattern' indicating the existence of spherulitic textures[20] and the pattern is elongated to the horizontal direction[21,22]. This is the typical behaviour of the deformation of perfect spherulites, as has been observed for polyethylene films. Based on the Hv scattering patterns, a model is proposed to analyse the orientational behaviour of crystallites within a polyethylene spherulite by using the method of Roe and Krigbaum[13–15]. In doing so, a mathematical representation of the orientation distribution function of crystallites must be given in terms of an expansion of the distribution function in a series of spherical harmonics by using the following three Cartesian coordinates.

*Figure 2* shows the geometrical interrelations of two Cartesian coordinates $0\text{–}X_1X_2X_3$ and $0\text{–}U_1U_2U_3$ fixed within the bulk specimen and crystallites, respectively. The orientation of the structural unit within the space of the film specimen may be specified by using three Euler angles $\phi$, $\theta$, $\eta$ as shown in *Figure 2a*. The angles $\theta$ and $\phi$, which define the orientation of the $U_3$ axis of the unit within the space, are the polar and azimuthal angles, respectively, and $\eta$ specifies the rotation of the unit around its own $U_3$ axis. The orientation of the $j$th axis with respect to the $0\text{–}X_1X_2X_3$ is given by the polar angle $\theta_j$ and the azimuthal angle $\phi_j$ as shown in *Figure 2b*. Moreover, the $j$th axis within the unit cell is specified by the polar angle $\Theta_j$ and $\Phi_j$ as shown in *Figure 2c*.

For a uniaxial system, the orientation distribution function $\omega(\cos\theta\eta)$ of polyethylene crystallites may be calculated from $2\pi q_j(\cos\theta_j)$ using a method proposed by Roe and Krigbaum[13,14].

$$F^j_{l0} = \langle P_l(\cos\theta_j)\rangle = \int_0^{2\pi}\int_0^{\pi} q_j(\cos\theta_j)P_l(\cos\theta_j)\sin\theta_j \,\mathrm{d}\theta_j \,\mathrm{d}\phi_j \tag{3}$$

$$2\pi q_j(\cos\theta_j) = \frac{1}{2} + \sum_{l=2}^{\infty}\frac{2l+1}{2}F^j_{l0}P_l(\cos\theta_j) \tag{4}$$

$$F^j_{l0} = F_{l00}P_l(\cos\Theta_j) + 2\sum_{n=2}^{l}\frac{(l-n)!}{(l+n)!}F_{l0n}P^n_l(\cos\Theta_j)\cos n\Phi_j \tag{5}$$

$$4\pi^2\omega(\cos\theta,\eta) = \frac{1}{2} + \sum_{l=2}^{\infty}\frac{(2l+1)}{2} \times \left\{F_{l00}P_l(\cos\theta) + 2\sum_{n=2}^{l}\frac{(l-n)!}{(l+n)!}F_{l0n}\cos n\eta\right\} \tag{6}$$

Here $l$ and $n$ are even integers. $P^n_l(x)$ and $P(x)$ are the associated Legendre and Legendre polynomials, respectively. The coefficient $F^j_{l0}$ and $F_{l00}$ may be represented by the coefficients $\alpha^j_{l0}$ and $A_{l0n}$ given by Roe and Krigbaum[17,18].

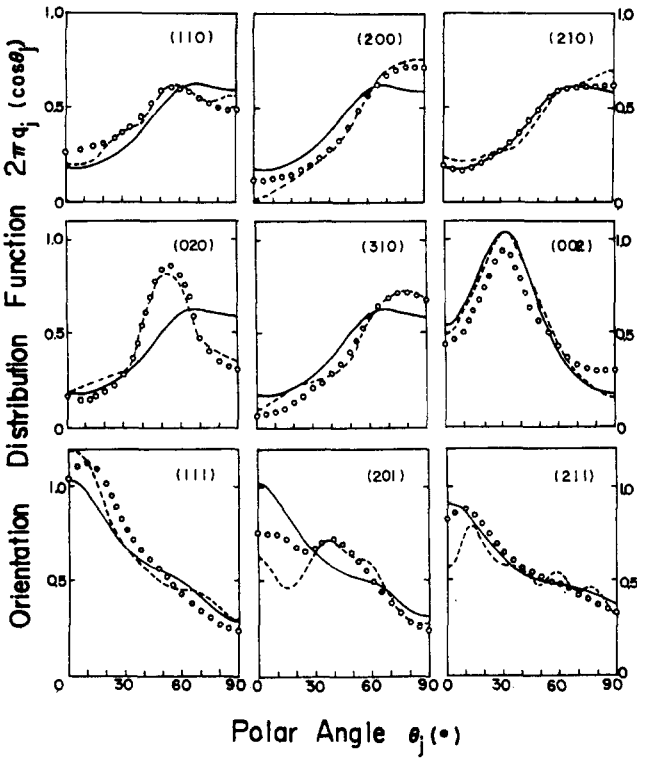


**Figure 3** Orientation distribution functions $2\pi q_j(\cos\theta_j)$ of the reciprocal lattice vectors of the indicated crystal planes of polyethylene melt films with = 1.5. Circles: values of $2\pi q_j(\cos\theta_j)$ obtained from experimental measurements. Dashed curves: calculated with the 17-term series (up to 16). Solid curve: $2\pi q_j(\cos\theta_j)$ calculated by using equations (10) and (13)

$$F^j_{l0} = \left\{\frac{2}{2l+1}\right\}2\pi\alpha^j_{l0} \tag{7}$$

$$F_{l0n} = \left\{\frac{2(l+n)!}{(2l+1)(l-n)!}\right\}4\pi^2 A_{l0n} \tag{8}$$

The coefficients $F_{l0n}$ can be determined by solving the linear equations represented by equation (5), since there exist more equations than the number of unknown, as was pointed out by Roe and Krigbaum[17]. Following Roe and Krigbaum, the values of $F_{l0n}$ were determined by the least-squares method. The calculation was continued until the best fit was achieved within the capability of the simplex method. Using the final values of parameters, a mean-square error between the calculated $F^j_{l0}$ and recalculated $F^j_{l0}$ was obtained using

$$R = \frac{\sum_j\sum_l \rho_j[(F^j_{l0})_{\mathrm{cal}} - (F^j_{l0})_{\mathrm{recal}}]^2}{\sum_j\sum_l[(F^j_{l0})_{\mathrm{cal}}]^2} \tag{9}$$

The values of weighing factors $\rho_j$, required in the least-squares calculation, were assigned somewhat subjectively on the assumption that the X-ray diffraction intensity is dependent upon the structure factor of each crystal plane. In this calculation, the weighing factors were assumed, as a first approximation, to be almost proportional to the structure factor and were subsequently modified to obtain the best fit between experimental and calculated results through numerical calculations by computer.

**Table 1** Direction of coordinate axes

| Coordinate system | Direction of coordinate of $X_i$, and $V_i$, and $U_i$ axes | |
|---|---|---|
| | $i = 1$ | $i = 3$ |
| $0-X_1X_2X_3$ | Normal to film surface | Stretching direction of film specimen |
| $0-V_1V_2V_3$ | Normal to lamellar surface containing $0V_2$ and $0V_3$ axes | Lamellar axis grown radially within a spherulite |
| $0-U_1U_2U_3$ | The $a$-axis of PE crystallite | The $c$-axis of PE crystallite |

**Table 2** Euler angles of coordinate transformations

| Reference coordinate | Euler angles | Oriented coordinates |
|---|---|---|
| $0-X_1X_2X_3$ | $\phi', \theta', \eta'$ | $0-V_1V_2V_3$ |
| $0-V_1V_2V_3$ | $\alpha, \beta, \gamma$ | $0-U_1U_2U_3$ |

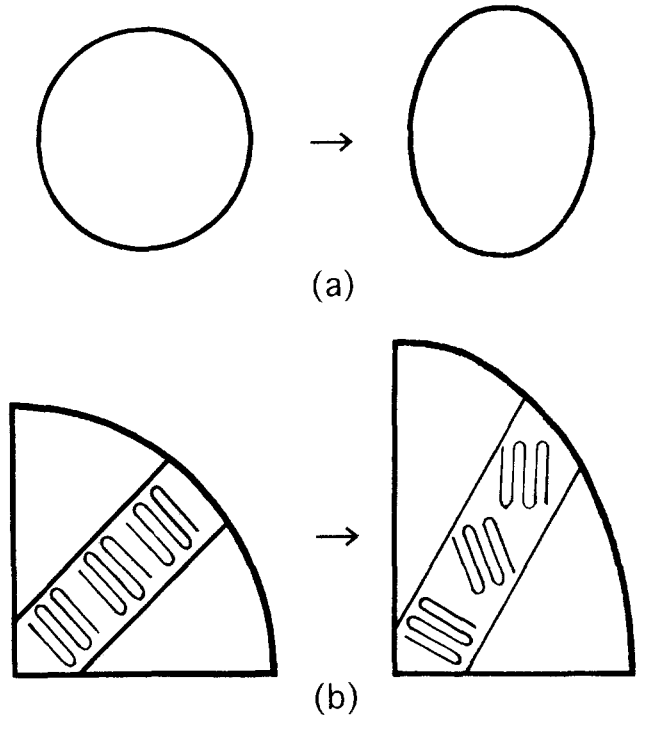


**Figure 4** Schematic illustration of deformation of polymer spherulites: (a) first step, deformation of spherical to ellipsoid structure; (b) second step, orientational mode of crystallites within a lamella

*Figure 3* compare the observed orientation distribution functions $2\pi q_j(\cos\theta_j)$ (open circles) with those (dashed curves) calculated for the respective crystal planes for the Sholex 5009 film with a draw ratio of $\lambda = 1.5$. The observed functions of the [1 1 0] and [2 0 0] directions have a peak at 58 and 90°, respectively, indicating the characteristic deformation behaviour of polyethylene spherulites. The function of the [0 0 2] direction (the $c$-axis) has a peak at 32° indicating the initial stage of crystal orientation. As discussed before, $F_{l0}^{j}$ were recalculated in turn from $F_{l00}$, which were initially determined by the weighted least-squares method, by the use of equation (5), and were further calculated $2\pi q_j(\cos\theta_j)$ from the recalculated $F_{l0}^{j}$ by the use of equation (4). As can be seen in the figure, fairly good agreement between the observed and calculated distribution functions was obtained for the less accurately measured crystal planes, the (3 1 0), (2 0 1) and (2 1 1) with lower weighting factor.

To study the deformation mechanism, a model relating crystal orientation to the orientation of lamellae was proposed and the distribution function of crystallites within the spherulite was assumed to be a function of lamellae. *Figure 4* shows a schematic illustration of the deformation of a spherulite proposed on the rheo-optical studies[23–26], in which model (a) shows instantaneous deformation of spherulite from spherulitic to ellipsoid structure and the model (b), orientation of crystallites within the oriented lamella as has been known as the second step.

*Tables 1* and *2* show the geometrical interrelations of three Cartesian coordinates $0-X_1X_2X_3$, $0-V_1V_2V_3$, and $0-U_1U_2U_3$ fixed within the bulk specimen, crystal lamella, and crystallites, respectively. The direction of the coordinate axes of each Cartesian coordinates are given in *Table 1* and the Euler angles of coordinate transformation among the three Cartesian coordinates are given in *Table 2*.

As the first step of the spherulite deformation, the instantaneous orientation of crystal lamellae including three kinds of rotation crystallites around crystal lamellar axis can be represented by the orientation of the Cartesian coordinates $0-V_1V_2V_3$, with respect to the Cartesian coordinates $0-X_1X_2X_3$ and can be formulated for uniaxial deformation as

$$\omega(\theta', \eta') = \frac{C_0}{8\pi^2}\omega(\theta')\{1 + \sigma_1(\lambda - 1)\cos^{2JA}\eta' + \sigma_2(\lambda - 1)\sin^{2JA}\eta' + \sigma_3\sin^2\theta'\cos^{2JA}\eta'\} \quad (10)$$

and

$$\omega(\theta') = \left[\frac{\sin^2\theta'\{2\sin^2\theta_0 - \sin^2\theta'\}}{\sin^4\theta_0} + fr\right]^{2JB} \quad (11)$$

where $\omega'(\theta', \eta')$ is an orientation distribution function of the crystal lamella with respect to the Cartesian coordinates $0-X_1X_2X_3$ and $\sigma_1$, $\sigma_2$, and $\sigma_3$ are parameters characterizing the ease of three kinds of instantaneous lamellar untwisting. Among them, $\sigma_1$ represents untwisting of lamellar surface assuring the orientation perpendicular to the plane $0-V_3X_3$ containing the stretching axis ($X_3$ axis) and lamellar axis ($V_3$ axis), while $\sigma_2$ represents untwisting of lamellar surface assuring the orientation parallel to the $0-V_3X_3$ plane. Both the rotations are independent of the position within the spherulite. $\sigma_3$ represents the same rotational mode as $\sigma_1$ but the rotation effect is considerable in the equatorial direction of the spherulite. JA is a parameter characterizing the sharpness of the three rotational modes. Here it should be noted that the three kinds of rotational modes have each different sharpness but the same parameter, JA, is chosen to avoid an increase in the number of parameters. $\omega(\theta')$ has a maximum for $\theta' = \theta_0$

indicating the preferential orientation of the rod axis at $\theta_0$. This function is given on the basis of the orientational behaviour of the $c$-axis having a maximum peak at around $\theta_j$ (see the function of the (0 0 2) plane in *Figure 3*) assuming that at low draw ratio such as $\lambda = 1.5$, most of the crystallites preserve the orientation in undeformed state. If this is the case, the preferential orientation of the $c$-axis may be approximated as $\theta_0 = \pi/2 - \theta_j$. This treatment is quite different from the affine fashion in the previous papers. Through a number of numerical calculations, however, it was found that when the affine function is employed, the orientation distribution of the $c$-axes has a maximum value at $\theta' = 0°$ denoting the preferential orientation with respect to the stretching direction in spite of the introduction of the complicated function concerning orientation function of crystallites. Hence equation (11) is given as a function to represent lamellar orientation to assure a peak around $\theta_j = 30°$. $C_0$ is a normalization constant defined by

$$\int_0^{2\pi}\int_0^{2\pi}\int_0^{\pi} \omega(\theta', \eta') \sin\theta' \mathrm{d}\theta' \mathrm{d}\phi' \mathrm{d}\eta' = 1 \qquad (12)$$

As the second step of the spherulite deformation, the delayed reorientation of crystallites (mosaic blocks) within the lamella, can be represented by the orientation of the Cartesian coordinates $0-U_1U_2U_3$, with respect to the Cartesian coordinates, $0-V_1V_2V_3$. The corresponding distribution function may be formulated as

$$q(\alpha, \beta, \gamma) = \frac{Q_0}{8\pi^2}[gr + \sigma_4 \sin^{2JG}\beta \cos^{2JC}\alpha \sin^{2JD}\gamma + \sigma_5(\lambda - 1)(\sin^4\theta' - \cos^4\beta + 2\cos^2\theta'\cos^2\beta) \times \cos^{2JE}\alpha \sin^{2JF}\gamma] \qquad (13)$$

In the undeformed state ($\lambda = 1$), equation (13) reduces to

$$q(\alpha, \beta, \gamma) = \frac{Q_0}{8\pi^2}[gr + \sigma_4 \sin^{2JG}\beta \cos^{2JC}\alpha \sin^{2JD}\gamma] \qquad (14)$$

$Q_0$ is a normalization constant defined by

$$\int_0^{2\pi}\int_0^{2\pi}\int_0^{\pi} q(\alpha, \beta, \gamma) \sin\beta \mathrm{d}\beta \mathrm{d}\alpha \mathrm{d}\gamma = 1 \qquad (15)$$

On the right side of equation (14), the first term corresponds to the fraction of crystallites within the lamella showing a random orientation. The second term corresponds to the fraction of crystallites with the $b$-axis oriented parallel to the lamellar axis; this term has a maximum value when the $b$- and $c$-axes are perfectly oriented in the direction of the lamellar axis ($V_3$ axis) and lamellar normal axis ($V_1$ axis), respectively. For example, JG in equation (13) is a parameter characterizing the sharpness of the distribution; i.e. JG = 0 means random orientation of the $c$-axis with respect to the lamellar axis and JG = $\infty$ means perfect orientation of the $c$-axis perpendicular to the lamellar axis. When JG = JC = JD = $\infty$, the $b$- and $c$-axes are perfectly oriented in the lamellar axis and lamellar normal axis, respectively.

In the deformed state, there is an additional component of orienting the $c$-axis of the crystallites parallel to the stretching direction. This is represented by the term $(\sin^4\theta' - \cos^4\beta + 2\cos^2\theta'\cos^2\beta)$ in equation (13) which has a maximum for $\beta = \theta'$ irrespective of the polar angle of lamellar orientation $\theta'$. This type of orientation is assumed to take place because of straining of the tie-chain molecules which causes the rotation of the crystallites around its own $a$-axis. The parameters JE and JF characterize the sharpness of the distribution function with respect to the angle $\alpha$ and $\gamma$, respectively. JE = 0 and JF = 0 mean the random orientation of crystallites around the $c$-axis.

By using the results in the previous reports[4–6], the orientation distribution function $2\pi q_j(\cos\theta_j)$ of a given reciprocal lattice vector of the $j$th crystal plane can be determined by the calculations

$$Q_{lsn}(\theta') = \int_0^{2\pi}\int_0^{2\pi}\int_0^{\pi} q(\alpha, \beta, \gamma) P_{lsn} \times (\cos\beta)\cos s\alpha \cos n\gamma \sin\beta \mathrm{d}\beta \mathrm{d}\alpha \mathrm{d}\gamma \qquad (16)$$

$$F'_{lsn} = \int_0^{2\pi}\int_0^{2\pi}\int_0^{\pi} \omega'(\theta', \eta') P_l^s(\cos\theta') Q_{lsn}(\theta') \times \cos s\eta' \mathrm{d}\theta' \mathrm{d}\eta' \mathrm{d}\phi' \qquad (17)$$

$$F_{l0n} = F'_{l0n} + 2\sum_{s=2}^{l} \frac{(l-n)!}{(l+n)!} F'_{lsn} \qquad (18)$$

$$F^j_{l0} = F_{l00} P_l(\cos\Theta_j) + 2\sum_{n=2}^{l} \frac{(l-n)!}{(l+n)!} F_{l0n} P_l^n(\cos\Theta_j)\cos n\Phi_j \qquad (19)$$

$$2\pi q_j(\cos\theta_j) = \frac{1}{2}\sum_{l=2}^{\infty} \frac{2l+1}{2} F^j_{l0} P_l(\cos\theta_j) \qquad (20)$$

The solid curves in *Figure 3* show the theoretical results calculated from equations (10) and (13) by using the values of parameters which were chosen to give the best fit between the experimental and theoretical results. The values chosen are $\sigma_1 = 0.955$, $\sigma_2 = 0.485$, $\sigma_3 = 1.51$, $\sigma_4 = 100$, $\sigma_5 = 0.01$, $fr = 0.1$, $gr = 0$, $\theta_0 = 32°$, JA = 1, JB = 40, JC = 1, JD = 1, JE = 5, JF = 3, and JG = 3. As can be seen in this figure, there is an individuality in the theoretical and experimental results for each plane and drastic deviation between the two results is not shown in the all crystal planes. The theoretical curves satisfy the characteristic profile having a peak at $\theta_j = 60°$ for the [1 1 0] direction and at $\theta_j = 30°$ for the [0 0 2] direction under the deformation of spherulites. Interestingly, the value of $\sigma_4$ is much larger than $\sigma_5$ in equation (13). This indicates that most of crystallites within the lamella preserve the original orientation even under elongation up to $\lambda = 1.5$ and few crystallites contribute to the delayed reorientation.

According to the previous models[4–6], the orientation of the lamellar axis was assumed to be affine and the calculated curve for the (0 0 2) plane did not have a peak at $\theta_j = 30°$ but a peak at $\theta_j = 0°$. Furthermore, the curve took negative values at most of the regions of $\theta_j$, since the orientation distribution function of crystallites within the lamella was obliged to give

$$q(\alpha, \beta, \gamma) = \frac{Q_0}{8\pi^2}[gr + \sigma_4 \cos^{2JG}\beta \cos^{2JC}\alpha \sin^{2JD}\gamma] + \sigma_5(\lambda - 1)(\sin^4\theta' - \cos^4\beta + 2\cos^2\theta'\cos^2\beta) \times \cos^{2JE}\alpha \sin^{2JF}\gamma - P(\theta')] \qquad (21)$$

where the term $P(\theta')$ is added to cancel out the variation of the constant $Q_0$ with the polar angle $\theta'$.

$$P(\theta') = \frac{1}{8\pi^2}\int_0^{2\pi}\int_0^{2\pi}\int_0^{\pi}(\sin^4\theta' - \cos^4\beta + 2\cos^2\theta'\cos^2\beta) \times \cos^{2JE}\alpha \sin^{2JF}\gamma \sin\beta \mathrm{d}\beta \mathrm{d}\alpha \mathrm{d}\gamma \quad (22)$$

We also confirmed that equation (21) takes negative value at some regions by the introduction of $P(\theta')$ and consequently $2\pi q_j(\cos\theta_j)$ becomes negative values at some parts of $\theta_j$. This causes the difficulty in doing the essential comparison between experimental and theoretical curves. Even so, the numerical calculation of equation (13) containing a constant $Q_0$ representing a complicated function of $\theta'$ was impossible by the simplex method[10]. The advance of computer technology, however, turned an impossibility into a possibility. Furthermore, it was found that the introduction of $P(\theta')$ causes a serious defect on the calculated Hv light scattering patterns, which shall be discussed later.

Here it should be noted that the concept to formulate equation (11) is based on the orientation distribution function of crystal grains by Fujita *et al.*[27]. In their calculation, the orientational relationship between crystallites and lamellae as a function is not taken into consideration directly and the relationship can be represented by a simple mathematical treatment where the angles $\alpha$, $\beta$ and $\gamma$ can be represented as $\theta'$ and $\phi'$. In this case, the calculated results are in good agreement with the observed ones. The same tendency was also confirmed for the direct representation of crystallite orientation within a bulk specimen[12].

Small angle light scattering from deformed three-dimensional spherulites has been studied by van Aartsen and Stein[28] assuming two kinds of density distributions of scattering elements within the spherulite deformed in an affine fashion. In their model system[28], the optical axes of the scattering element is tilted towards the spherulite radius in the longitudinal zone and is rotated around the radius in the lateral zone of the deformed spherulite. In another treatment, Hv light scattering from a deformed three-dimensional spherulite was formulated by using equation (21)[29]. Similar treatment has already been reported for nylon 6 spherulite[5]. Namely, the patterns were calculated by using the values of parameters to give the best fit between the theoretical and observed curves of their reciprocal lattice vectors of the crystal planes for polyethylene[29] and nylon 6 spherulites[5]. Here it should be noted that the four-leaf pattern in an undeformed polyethylene spherulite transformed eight-leaf pattern can be distinguished even at an extension ratio as small as $\lambda = 1.1$[29]. Such an eight-leaf pattern was found to be due to the fact that the upper lobe had a positive amplitude, while the lower lobe had a negative amplitude. This phenomenon did not arise when the parameter denoting the orientation of crystallites within the lamella was zero, which corresponded to $\sigma_5 = 0$ in the present model system. The negative value of the amplitude giving the eight-leaf pattern in the previous papers[5,29] was thought to be due to the introduction of $P(\theta')$. To check the origin of the disagreement between the theoretical and observed patterns, the numerical calculations were carried out by using equations (10) and (13).

To simplify the present model system, the spherulite was assumed to be an affine deformation. The scattered intensity $I(\theta, \mu)$ is given by

$$I(\theta, \mu) = [E(\theta, \mu)]^2 \quad (23)$$

where the angle $\theta$ (different from $\theta$ in *Figure 3*) and $\mu$ are the scattering and azimuthal angles. The quantity $E(\theta, \mu)$ is the amplitude of the scattered ray given by

$$E(\theta, \mu) = E_0\int_0^{R(\theta')}(\mathbf{M}\cdot\mathbf{O})N(\theta', \phi', r) \times \cos[k(\mathbf{r}\cdot\mathbf{s})r^2 \sin\theta' \mathrm{d}r\mathrm{d}\theta'\mathrm{d}\phi' \quad (24)$$

where $(\mathbf{M}\cdot\mathbf{O})$ in equation (24) is given by

$$(\mathbf{M}\cdot\mathbf{O}) = \int_0^{2\pi}\int_0^{\pi}(\alpha_3 - \alpha_1)(\mathbf{u}_3\cdot\mathbf{x}_3)(\mathbf{u}_3\cdot\mathbf{x}_2) \times \left[\int_0^{2\pi} q(\alpha, \beta, \gamma)\mathrm{d}\gamma\right]\sin\beta \mathrm{d}\beta\mathrm{d}\alpha \quad (25)$$

where $(\mathbf{M}\cdot\mathbf{O})$ is the scalar product of the induced dipole moment $\mathbf{M}$ in a given lamella and the unit vector $\mathbf{O}$ along the polarization direction of the analyzer, $\mathbf{r}$ is the position vector along the radial direction. $\mathbf{s}$ is the vector defined by $(\mathbf{s}_0 - \mathbf{s}')$, where $\mathbf{s}_0$ and $\mathbf{s}'$ are unit vectors parallel to the propagation directions of the incident and scattered beams, respectively; $\mathbf{u}_3$ is the vector along the optical axis (the $c$-axis); $\mathbf{x}_3$ and $\mathbf{x}_2$ are the vectors along the $X_3$ and $X_2$ directions, respectively; $\alpha_3$ and $\alpha_1$ are the polarizabilities of the scattering element parallel and perpendicular to the principal optical axis, respectively. $N(\theta', \phi', r)$ is the density distribution function of the scattering elements; $r$ is the position vector; $k$ denotes $2\pi/\lambda'$; and $\lambda'$ is the wavelength of the light within the specimen. $R(\theta')$ in equation (24) is the radius of the deformed spherulite at a given polar angle $\theta'$, and is given by the following equation on the basis of affine deformation and constant volume of the spherulite during uniaxial deformation

$$R(\theta') = \lambda R_0/[\lambda^3 - (\lambda^3 - 1)\cos^2\theta']^{1/2} \quad (26)$$

Here $R_0$ is the spherulite radius in the undeformed state. $R(\theta')$ was introduced to represent affine deformation of the spherulite, although the orientation of crystal lamellae given as equation (10) is independent of the deformation of the spherulite with an affine fashion.

For the undeformed spherulite, the density distribution $N(\theta', \phi', r)$ may be assumed to be uniform, independent of angles $\theta'$ and $\phi'$ and of position $r$ within the spherulite. For the deformed spherulite, it is given by

$$N(\theta', \phi', r) = \frac{3C_0}{8\pi^2}(1 + \Delta F) \quad (27)$$

where $C_0$ is a normalization constant. The additional term $\Delta F$ takes into account the effect of the untwisting of lamella

$$\Delta F = 1 + \sigma_1(\lambda - 1)\cos^{2JA}\eta' + \sigma_2(\lambda - 1)\sin^{2JA}\eta' + \sigma_3\sin^2\theta'\cos^{2JA}\eta' \quad (28)$$

The scattered intensity was calculated as a function of $R_0/\lambda'$ and was taken as 10. Before carrying out the numerical calculations to evaluate the scattered intensity,

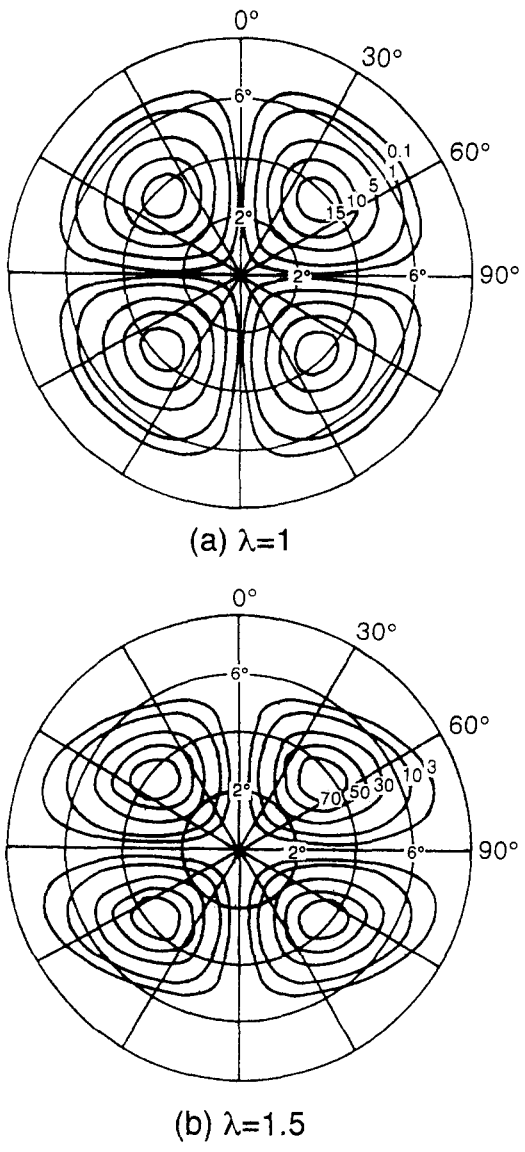


**Figure 5** Calculated intensity distribution of the Hv light scattering: (a) from an undeformed spherulite and (b) a deformed spherulite with $\lambda = 1.5$

the amplitude in equation (24) was normalized by $R_0{}^3$. *Figure 5* shows the calculated patterns for values of the parameters identical with those in *Figure 3*. In the undeformed state, the typical four-leaf clover pattern having intensity maxima at azimuthal angles of multiples of 45° will be noted. The calculated result at $\lambda = 1.5$ shows four-leaf pattern whose lobes are extended in the horizontal direction and the scattered intensity becomes more intense than that of the pattern in the undeformed state. These patterns are in good agreement with the patterns observed by the elongation of films with perfect three-dimensional spherulites. The lobe has a positive amplitude and any eight-leaf pattern is not obtained. Accordingly, it turns out that the eight-leaf pattern by the introduction of $P(\theta')$ is only artificial.

The above calculations take account only of the crystalline orientation within the deformed spherulite and omit contributions from other factors, such as orientation and density fluctuations of the crystals, size distribution of spherulites and noncrystalline orientation effects including the anisotropy of the surrounding medium. However, it may be expected that these contributions do not cause significant effects on the profile of Hv patterns in the present experimental specimens with perfect spherulites with high crystallinity.

## CONCLUSION

To study the deformation mechanism of polyethylene spherulites, high density polyethylene melt films were used as test specimens. The orientation distribution functions of the reciprocal lattice vectors for nine crystal planes were measured by X-ray diffraction techniques and small angle light scattering under Hv polarization condition. Based on the functions, a model was proposed. In this model system, two steps in the deformation mechanism were assumed: (1) instantaneous deformation of the spherulite associated with orientation of lamellar axis and rotation of lamella around the lamellar axis; (2) orientation of crystallites within the oriented lamella. Thus the distribution function for orientation of crystallites within crystal lamella is assumed to be a function of lamellar orientation. The formulation is similar to that reported already. However, any unrigorous terms to avoid complicated treatment were not introduced in this paper. The orientation distribution functions of the reciprocal lattice vectors calculated were in good agreement with those observed. Furthermore, Hv light scattered intensity distribution in an undeformed state showed that the typical four-leaf clover pattern and the scattering lobes were extended in the horizontal direction indicating the deformation from spherical to ellipsoid structure.

## REFERENCES

1. Sasaguri, K., Yamada, H. and Stein, R. S., *J. Appl. Phys.*, 1964, **35**, 3188.
2. Oda, T., Nomura, S. and Kawai, H., *J. Polym. Sci., Part A*, 1965, **3**, 1993.
3. Nomura, S., Asanuma, A., Suehiro, S. and Kawai, H., *J. Polym. Sci., Part A-2*, 1971, **9**, 1991.
4. Nomura, S., Matsuo, M. and Kawai, H., *J. Polym. Sci. Polym. Phys. Ed.*, 1972, **10**, 2489.
5. Matsuo, M., Hattori, H., Nomura, S. and Kawai, H., *J. Polym. Sci. Polym. Phys. Ed.*, 1976, **14**, 223.
6. Matsuo, M., Hirota, K., Fujita, K. and Kawai, H., *Macromolecules*, 1978, **11**, 1000.
7. Hay, I. L. and Keller, A., *Kolloid-Z.Z. für Polym.*, 1965, **204**, 43.
8. Kobayashi, K. and Nagasawa, T., *J. Polym. Sci. Part C*, 1966, **15**, 163.
9. Samuels, R. J., *J. Polym. Sci., Part C*, 1966, **13**, 37.
10. Spendly, W., Hext, G. K. and Himsworth, F. R., *Technometrics*, 1962, **4**, 441.
11. Sugiura, Y. and Matsuo, M., in preparation.
12. Matsuo, M., Ooki, J., Harashina, Y., Ogita, T. and Manley, R. S. T., *Macromolecules*, 1995, **28**, 4951.
13. Erman, B., Bahar, I., Kloczkowski, A. and Mark, J. E., *Macromolecules*, 1990, **23**, 5335.
14. Bahar, I., Erman, B., Kloczkowski, A. and Mark, J. E., *Macromolecules*, 1990, **23**, 5341.
15. Flory, P. J., *Proc. R. Soc. London, Ser, A*, 1974, **234**, 73.
16. Flory, P. J. and Ronca, G., *Mol. Cryst. Liq. Cryst.*, 1979, **54**, 289, 311.
17. Roe, R. J. and Krigbaum, W. R., *J. Chem. Phys.*, 1964, **40**, 2608.
18. Krigbaum, W. R. and Roe, R. J., *J. Chem. Phys.*, 1964, **41**, 737.
19. Roe, R. J., *J. Appl. Phys.*, 1965, **36**, 2024.
20. Stein, R. S. and Rhodes, M. B., *J. Appl. Phys.*, 1960, **31**, 1873.
21. Motegi, M., Oda, T., Moritani, M. and Kawai, H., *Polymer J.*, 1970, **1**, 209.
22. Clough, S. B., van Aartsen, J. J. and Stein, R. S., *J. Appl. Phys.*, 1965, **36** 3072.

23. Sasaguri, K., Hoshino, S. and Stein, R. S., *J. Appl. Phys.*, 1964, **35**, 47.
24. Oda, T. and Stein, R. S., *J. Polym. Sci. A-2*, 1972, **10**, 685.
25. Suehiro, S., Yamada, T., Inagaki, H., Kyu, T., Nomura, S. and Kawai, H., *J. Polym. Sci. Polym. Phys. Ed.*, 1979, **17**, 763.
26. Suehiro, S., Kyu, T., Fujita, K. and Kawai, H., *Polymer J.*, 1979, **11**, 331.
27. Fujita, K., Suehiro, S., Nomura, S. and Kawai, H., *Polymer J.*, 1982, **14**, 545.
28. van Aartsen, J. J. and Stein, R. S., *J. Polym. Sci. A-2*, 1971, **9**, 295.
29. Nomura, S., Matsuo, M. and Kawai, H., *J. Polym. Sci. Polym. Phys. Ed.*, 1974, **12**, 1371.